

FIELD EVALUATION OF ALTERNATIVE ISOLATION JOINTS AT O'HARE  
INTERNATIONAL AIRPORT

By:

Jacob Henschen, Armen Amirkhanian, Jeffery Roesler, David Lange

Department of Civil and Environmental Engineering

University of Illinois Urbana-Champaign

Urbana, Illinois 61801 USA

[jhensche@illinois.edu](mailto:jhensche@illinois.edu)

[amirkha1@illinois.edu](mailto:amirkha1@illinois.edu)

[jroesler@illinois.edu](mailto:jroesler@illinois.edu)

[dlange@illinois.edu](mailto:dlange@illinois.edu)

PRESENTED FOR THE 2014 FAA WORLDWIDE AIRPORT TECHNOLOGY TRANSFER  
CONFERENCE

Galloway, New Jersey, USA

August 2014

## ABSTRACT

Airfield isolation joints are specified to separate horizontal movement between two adjacent concrete pavements. Typically, these are a thickened edge joint without any man-made connection, which requires a 25% thicker slab to compensate for the higher free edge stresses. Thickened edge joints are more difficult to construct and thus require more time and resources to complete. Recently, the FAA introduced an alternative design for isolation joint with embedded steel reinforcement near the slab bottom allowing the normal slab thickness to be maintained. In this study, two isolation joint types were constructed at Chicago O'Hare International Airport. One section followed the recently recommended FAA steel reinforcement design and the other section was constructed with macro-fiber reinforced concrete. Embedment gages were placed in the freshly cast concrete as well as gages on the steel reinforcing bars to monitor the strains under aircraft loading. Dynamic strain data was collected during a night of aircraft taxiing over the joint. In addition, heavy weight deflectometer (HWD) testing was conducted at a separate time to measure the isolation joint effectiveness. The alternate joint designs were modeled using 2D finite element analysis for comparison to the experimental results and to determine the critical tensile stresses. The field analysis indicates that the steel or macro-fiber reinforced joint design with a stabilized base should prevent the tensile stresses in the pavement from causing premature failure of the concrete isolation joint.

## INTRODUCTION

Isolation joints allow for adjacent slabs to move in independent directions and prevent damage associated with connected slabs thermal or moisture movements. Isolations joints are common on airfields where, for example, a concrete taxiway intersects an existing runway and must accommodate orthogonal movements. These transverse deformations restrict the use of dowel bars across this type of joint, which results in free edge stresses in both sets of slabs. The American Concrete Pavement Association (ACPA) suggests a thickened edge joint design is specified in order to accommodate the higher stresses [1, 2]. With a thickened edge, the tensile stresses in the concrete are reduced by an increased slab thickness.

In airfield pavements, the FAA standards provide two alternate isolation joint designs [3]. Type A is a thickened edge where the slab thickness is increased by 25% at and near the free edge. While this joint type is the most commonly used, it is also expensive to construct because of the non-uniform cross-section. The non-uniform cross-section requires changing the grade of the base and subgrade relative to the rest of the pavement grading. Additionally, buried conduits or drainage structures may make this joint design impossible or prohibitively expensive. As a result, the FAA recently introduced an alternate isolation joint design, Type A-1, with a uniform concrete slab cross-section and steel reinforcement near the bottom of the slab to provide post-crack load carrying capacity. Figure 1 depicts both types of isolation joints. The number and size of the reinforcing bars is determined by the aircraft type and loading. A reinforced joint is easier to construct than a thickened edge, but there is limited data on its performance under live aircraft

loading. Recently, response and failure testing was conducted at the National Airport Pavement Test Facility (NAPTF) to compare both isolation joint types, and the preliminary results as reported by Blotta et al. have focused on the free edge strains and apparent load transfer efficiency [4].

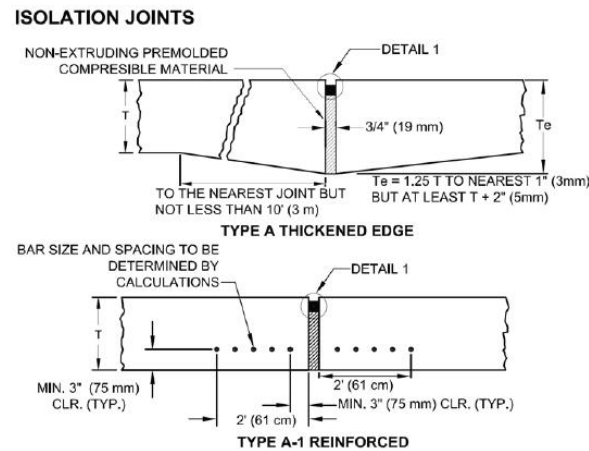


Figure 1. Airfield isolation joint design alternatives [3].

The purpose of this research project was to determine the in-situ performance of the steel reinforced isolation joint (Type A-1). The test site is a taxiway tie-in located at O'Hare Airport in Chicago, Illinois (Figure 2). Several slab panels adjacent to the isolation joint were constructed using eight #6 reinforcing bars per the FAA standard. Additionally, several uniform cross-section panels were constructed using synthetic macro-fiber reinforcement in the concrete, at a dosage of 7 lb/yd<sup>3</sup> (0.4% by volume), as an alternative to the isolation joint with transverse steel. Strain gages were embedded in each isolation joint type to gather response data during aircraft loading. The measured strains were compared to those generated from a finite element analysis using ILLI-SLAB [5]. Finally, heavy weight deflectometer (HWD) testing was performed to supplement the joint responses measured with live aircraft traffic.

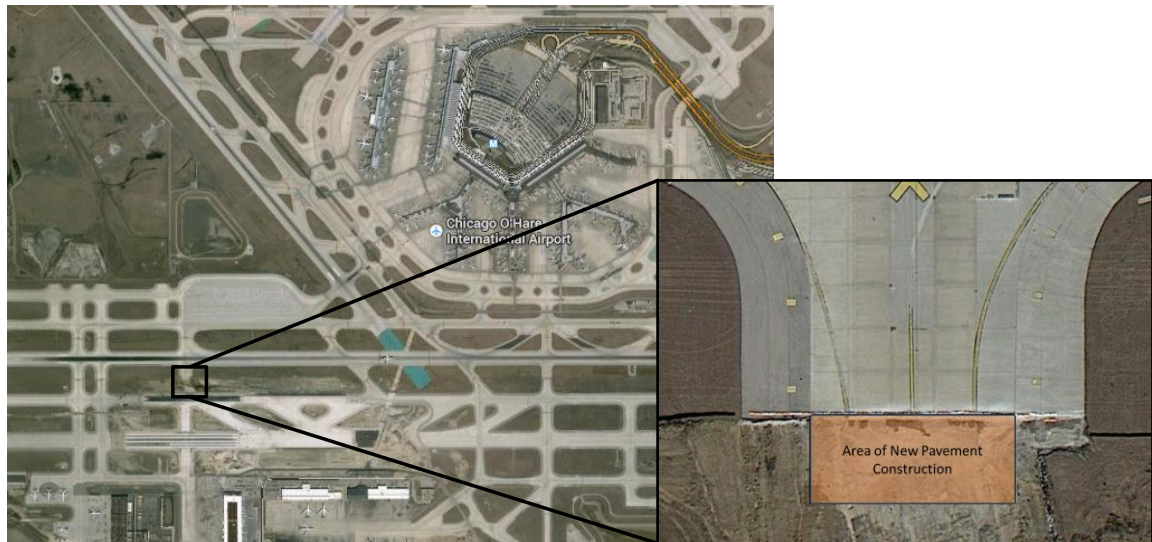


Figure 2. Test site for isolation joint instrumentation.

## FIELD TEST PLAN

For the field response testing, measuring the strain in the concrete and steel reinforcement was necessary. Concrete strains were obtained with 120 ohm quarter bridge strain gages measuring 2.5 in. long (Figure 3). Brackets positioned the embedment gages 2 in. from the upper and lower surfaces of the slab and parallel to the isolation joint (Figure 4). The brackets were designed to suspend the gages at specific elevations without interfering with the measurements. The positions along the isolation joint were selected to be in the areas of high stress based on preliminary ILLI-SLAB analysis of the aircraft types expected to traverse the joint. Due to the variability in aircraft type, loading, and gear configuration, the modeling only accounted for the Boeing 747-8 and 777-200 which were chosen based on their high maximum takeoff weight (MTOW). To allow for adequate concrete cover, the embedment gages were offset 3 in. from the vertical face of the isolation joint. One bracket was used on both sides of the taxiway centerline and on both sides of the isolation joint for a total of 4 brackets with 2 gages per bracket (Figure 5).

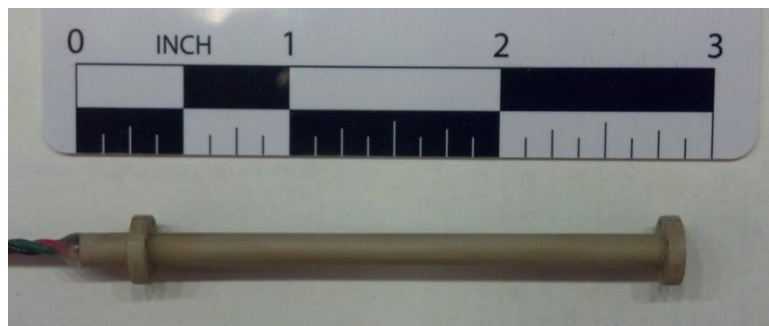


Figure 3. Concrete embedment strain gage.



Figure 4. Mounting bracket for concrete embedment gages.

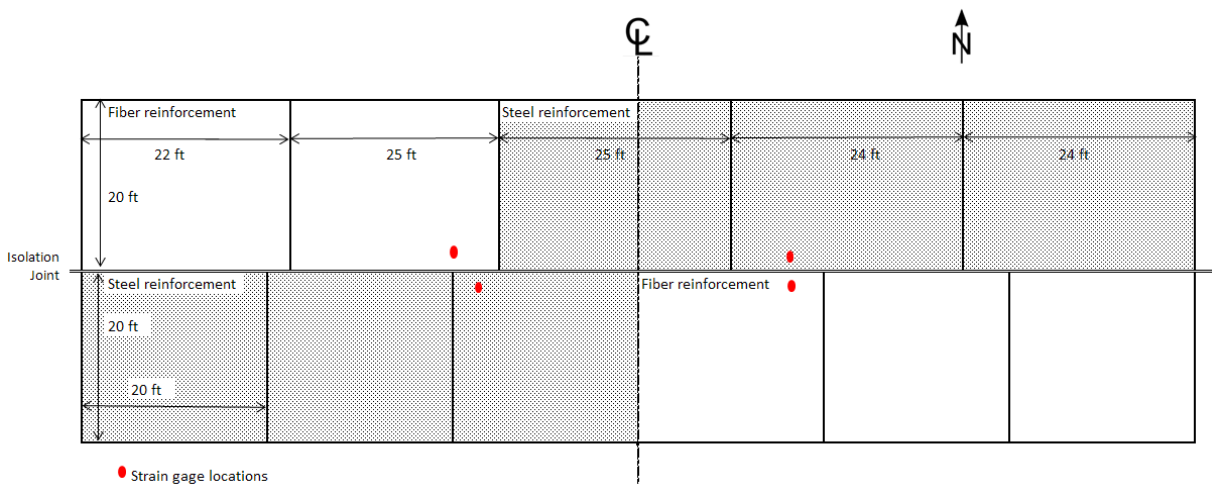


Figure 5. Plan view of strain gage locations.

For measurements on the steel reinforcement, foil strain gages were fixed directly to the reinforcing bars (Figures 6 and 7). The gages on the steel were approximately 3 in. from the bottom of the slab and were at the same positions as the embedment gages along the isolation joint. In each slab with reinforcement, gages were placed on the two reinforcing bars nearest the isolation joint. The reinforcement gages could confirm whether or not the concrete has begun to crack at the bottom of the slab and the validity of the concrete strain measurements. Cracks intersecting or near the steel strain gages would significantly change its output relative to the concrete embedment gages.

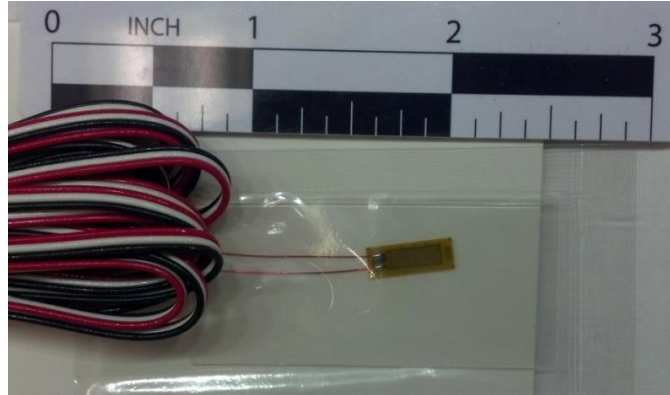


Figure 6. Foil strain gage to be mounted on steel reinforcement.



Figure 7. Foil strain gages fixed to reinforcement.

Data was collected using the University of Illinois (UIUC) Mobile Research Laboratory which was positioned on the airfield near the isolation joint. The laboratory housed a data acquisition system which allowed the sensors to be actively monitored and triggered while aircraft traversed the joint (Figure 8). The temporary nature of this laboratory allows for rapid deployment of the data acquisition system and periodic data collection sessions.





Figure 8. University of Illinois mobile research laboratory with aircraft passing instrumented taxiway.

## FIELD RESULTS

The first data collection session with aircraft loading occurred on November 11, 2013. A schematic of the instrumented slab section is presented in Figure 9. The location of the strain gauges on the east side relative to the centerline mirrored the west side locations. During the nighttime data collection, three different aircraft types (MD-11, A300-600, DC-10) traversed the section for a total of five passes (Table 1). The data from the strain gauges was sampled at 800 Hz as shown in Figure 10. Due to low visibility and safety zone concerns, there was limited time to access the sensor wires and thus the strain gauges mounted on the east side of the taxiway were not acquired.

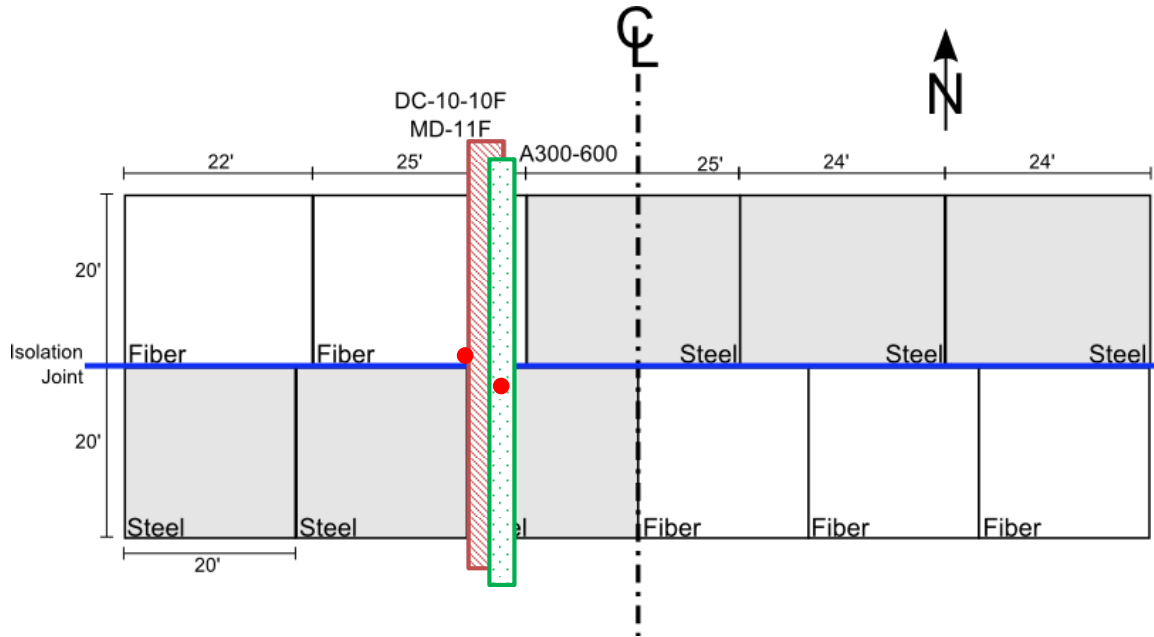


Figure 9. Schematic of instrumented slabs on Taxiway DD. The red dots indicate the strain gage locations. The colored shaded section indicates the gear travel path of the associated aircraft assuming aircraft centerline coincides with pavement the centerline. Figure is to scale.

Table 1.

Peak tensile strain for each aircraft loading. The order of aircraft indicates the sequence passing the test section.

Flight Number	Tail Number	Aircraft Type	Peak Fiber Section Strain ( $\mu\epsilon$ )	Peak Steel Section Strain ( $\mu\epsilon$ )	Peak Rebar Strain ( $\mu\epsilon$ )
FDX1950	N741FD	A300B4-622R	7.6	18.9	16.0
FDX1706	N396FE	DC-10-10F	24.8	14.3	13.4
FDX1447	N592FE	MD-11F	11.5	22.9	20.4
FDX1157	N40061	DC-10-10F	10.0	21.3	18.2
FDX1405	N392FE	DC-10-10F	11.7	20.3	21.5

## COMPARISON TO ILLI-SLAB

The tensile strains listed in Table 1 were measured directly from the pavement sensors. The peak fiber strain and steel strain came from the embedded concrete gage in the fiber reinforced concrete and steel reinforced section, respectively. The rebar strain was output from the foil gage on the steel reinforcement. The strains from the top and bottom embedment gauges generally matched one another indicating that the gauges remained intact during construction and their vertical position was not altered. ILLI-SLAB was used to run cases to compare theoretical strains with the field measured strains. Several assumptions were made because of the uncertainty in the various pavement layer properties (Table 2). The base layer consisted of 6 inches of dense



graded asphalt concrete on top of a 6 inch open-graded asphalt layer. For this analysis, deflection load transfer efficiency (LTE) across the dowelled contraction and construction joints were assumed to be 93%, which is similar to measured LTE at O'Hare for the recently constructed 9L-27R concrete pavement structure. The LTE across the isolation joint was initially assumed to be zero. The exact aircraft weights were not known and it was assumed that the aircraft were at 87 percent of their listed maximum landing weight (MLW) based on guidance from FedEx, which was the operator of all the aircraft that traversed the instrumented section. Other aircraft characteristics were obtained from manufacturer technical documents (Table 3) [6-8]. It was assumed that the gages were at the exact height as when they were installed and no movement of the gage occurred during construction.

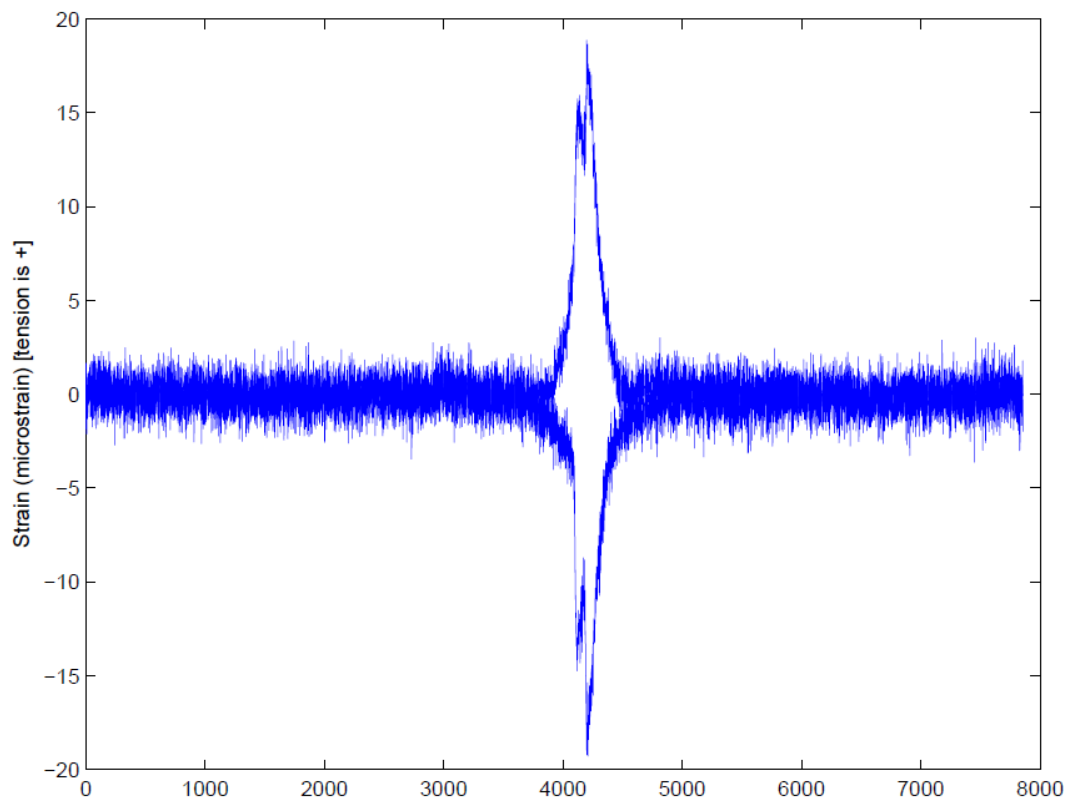


Figure 10. Recorded strain from the SW embedment gage tree as the A300-600 aircraft traversed the section.

Table 2.

Design assumption used in ILLI-SLAB analysis.

Property	Value
Elastic Modulus (concrete)	$6.0 \times 10^6$ psi
Elastic Modulus (asphalt base)	$4.5 \times 10^5$ psi
Subgrade Reaction, k	75 pci
Load Transfer Efficiency	93%
Concrete Thickness	18 in
Asphalt Thickness	12 in
Poisson Ratio (concrete)	0.15
Poisson Ratio (asphalt base)	0.35

Table 3.

Aircraft characteristics used in modeling pavement loading.

Aircraft Type	87% of MLW (lbs)	Tire Pressure (psi)	Wheel Spacing (in)	Axle Spacing (in)
A300B4-622R	268,526	194	36.5	55.0
DC-10-10F	316,245	195	54.0	64.0
MD-11F*	410,205	206	54.0	64.0

\*The belly gear was considered in the weight distribution but not in the model.

The ILLI-SLAB analysis determined the position of the aircraft relative to the centerline that minimized the difference between the measured and calculated strain. Based on the ILLI-SLAB analysis, it appears that the aircraft travelled closely along the taxiway centerline with little deviation (Table 4) with exception of event FDX1706. The peak tensile stress at the edge of the slab along the isolation joint was then determined from ILLI-SLAB (Table 5). Furthermore, a series of ILLI-SLAB runs was conducted on a theoretical thickened edge slab of 22.5 inch thickness. These results are presented in Table 6. The fiber, 25 foot by 20 foot, and steel, 20 foot by 20 foot, section stresses are not different because of the reinforcement scheme chosen, but their differing slab geometry as shown in Figure 9. The results in Table 6 are the worst case scenario assuming no structural support outside of the free edge at the isolation joint. With a sufficiently strong base layer, there will be foundation support beyond the free edge which will provide some level of structural load transfer.

Table 4.

Strain data from field measurements. Results were used to match a series of ILLI-SLAB runs in order to validate the readings. Deviation directions are given as East (E) and West (W) from centerline.

Flight Number	Aircraft	Fiber Section Embedded ( $\mu\epsilon$ )	Fiber Section ILLI-SLAB ( $\mu\epsilon$ )	Steel Section Embedded ( $\mu\epsilon$ )	Steel Section ILLI-SLAB ( $\mu\epsilon$ )	Deviation (ft)
FDX1950	A300B4-622R	7.6	7	18.9	19	1.5, W
FDX1706	DC-10-10F	24.8	22	14.3	9	6.0, E
FDX1447	MD-11F	11.5	12	22.9	24	2.5, E
FDX1157	DC-10-10F	10.0	8	21.3	22	2.0, E
FDX1405	DC-10-10F	11.7	8	20.3	22	2.0, E

Table 5.

Calculated peak tensile stresses for the various aircraft loadings. Peak stress was taken along the free edge of the isolation joint.

Flight Number	Aircraft	Peak Tensile Stress on [25'x20'] Section (psi)	Peak Tensile Stress on [20'x20'] Section (psi)
FDX1950	A300B4-622R	479	526
FDX1706	DC-10-10F	266	262
FDX1447	MD-11F	301	315
FDX1157	DC-10-10F	332	341
FDX1405	DC-10-10F	332	341

Table 6.

Calculated peak tensile stresses for the various aircraft loadings for a thickened edge isolation joint.

Flight Number	Aircraft	Peak Tensile Stress on Thickened Section [25'x20'] (psi)	Peak Tensile Stress on Thickened Section [20'x20'] (psi)
FDX1950	A300B4-622R	335	365
FDX1706	DC-10-10F	185	182
FDX1447	MD-11F	212	220
FDX1157	DC-10-10F	233	237
FDX1405	DC-10-10F	233	237

Heavy weight deflectometer (HWD) testing was conducted on the isolation joint on September 9, 2013. Three different loads levels were used at 5 different drop locations across the isolation joint with the load transfer efficiency for each drop presented in Table 7. Each drop location is outlined in Figure 10. Despite no physical connections exists between the adjacent

concrete slabs, the isolation joint had an average deflection load transfer efficiency of 76% (56,000 lb load level). The deflection was transferred between adjacent slabs through the asphalt concrete base layers since there is no other deflection transfer mechanism present. Using the HWD joint data, a re-analysis in ILLI-SLAB of the critical loading case (A300-622R) was performed and the results are presented in Table 8. The average LTE was inputted into ILLI-SLAB as a joint stiffness of 43,000 psi. Both isolation joint types exhibit very low tensile stresses upon loading. The stiff base layer provides structural support at the isolation joint further reducing the bending stresses shown in Tables 5 and 6. The tensile stresses for the Type A-1 and fiber reinforced concrete isolation are less than 50% of the concrete flexural strength and thus no fatigue cracking is expected during the design life of this taxiway from these aircraft loadings. The only cracking that may occur is volume restraint of the concrete as a result of the steel reinforcement. This initial testing and analysis provides additional evidence that a Type A-1 isolation joint of uniform concrete thickness, whether it contains reinforcing steel near the bottom of the slab or only macro-fibers, provides adequate load carrying capacity relative to the standard thickened edge joint especially in conjunction with a stiff stabilized base layer.

Table 7.  
HWD deflection load transfer testing data at isolation joint.

Drop 1		Drop 2		Drop 3		Drop 4		Drop 5	
Load (lb)	LTE	Load (lb)	LTE	Load (lb)	LTE	Load (lb)	LTE	Load (lb)	LTE
15288	80%	15235	77%	15277	82%	15255	82%	15398	76%
34346	77%	34394	75%	34335	81%	34677	80%	34635	74%
56699	74%	56827	73%	56393	80%	56846	79%	57326	72%

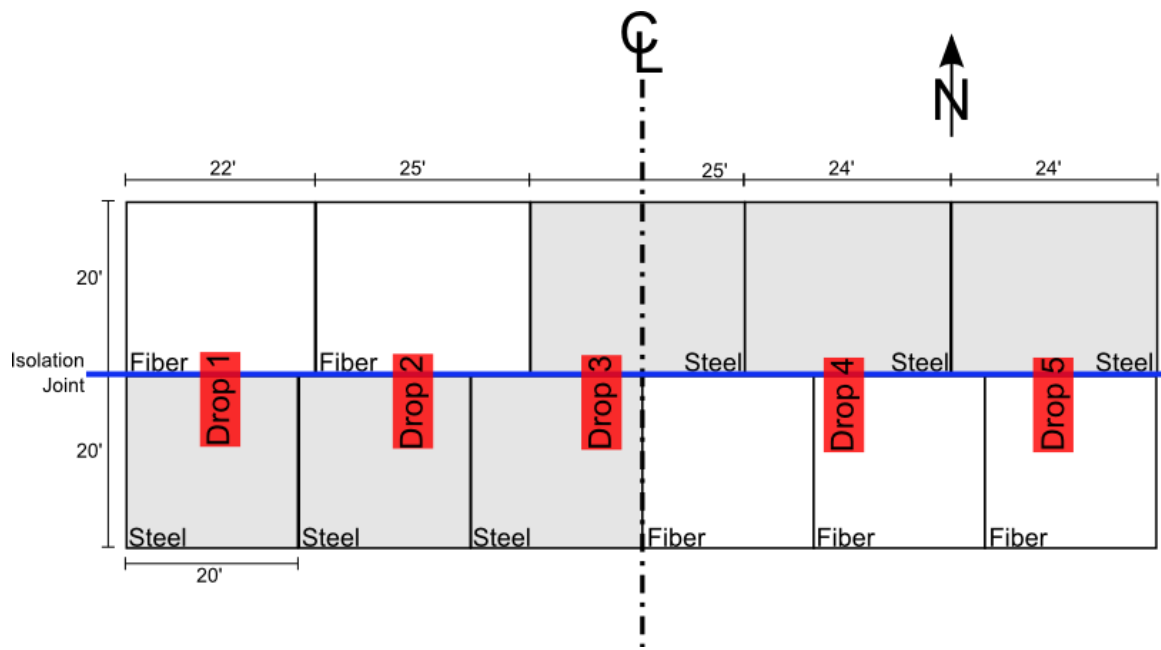


Figure 11: Location of HWD testing on instrumented section. Red areas indicate the drop basins.

Table 8.

Re-analysis of A300-622R aircraft loading incorporating HWD data.

Loading Case	Peak Tensile Stress (psi)
Fiber Section	301
25' Section Thickened Edge	214
Steel Section	331
20' Section Thickened Edge	235

## CONCLUSIONS

Two new isolation joints were constructed at Chicago O'Hare airport to determine if they could routinely be constructed to replace the more expensive thickened edge isolation joint. Type A-1 steel reinforced and macro-fiber isolation joints were constructed with a uniform concrete thickness that matches the concrete thickness on the remaining taxiway. Concrete embedment and steel strain gages measured the response of the concrete slabs near the isolation joint as live aircraft traversed the joint. The field response data were used to compare alternative isolation joint designs to theoretical model results. The bending strains in the concrete and steel obtained from the field showed the aircraft were approximately centered on the taxiway and the measured responses are similar to 2D plate theory analysis. The similarity in measured strain in the concrete and on the steel reinforcement bars suggested that the concrete pavement had not experienced cracking at the bottom of the slab at the time of testing.

HWD testing demonstrated that the asphalt stabilized base layer significantly contributed to deflection transfer across the isolation joint. Synthesis of the field and theoretical analysis indicated that the steel reinforced or macro-fiber reinforced isolation joint should provide the same performance as the traditional thickened edge joint during the taxiway's design life. Both types of joints produced low tensile stresses relative to the concrete flexural strength. The incorporation of the stiff base layer under the slab partially transfer some of the stress across the isolation joint through the base layer despite an apparent free edge condition. The construction of future alternative isolation joints with uniform concrete thickness, whether with macro-fiber reinforced concrete or a Type A-1 steel reinforcement design, should employ a stabilized base layer to share and reduce the tensile stresses in the concrete slabs at this free edge loading condition.

## ACKNOWLEDGEMENTS

The authors would like to acknowledge the O'Hare Modernization Program for providing research funds and Ross Anderson of Bowman, Barrett & Associates Inc. for coordinating the sensor installation and data collection. The authors would also like to thank Dr. David Brill of the FAA Airport Pavement Technology R&D Branch for providing guidance in planning the sensor installation. The HWD data was provided by ERI, Inc.

## REFERENCES

1. ACPA, "Proper Use of Isolation and Expansion Joints in Concrete Pavements," American Concrete Pavement Association, Skokie, Illinois, pp 1-2, 1992.
2. Jung, Y.; Zollinger, D.; and Tayabji, S., "Best Practices of Concrete Pavement Transition Design and Construction," Publication FHWA/TX-07/0-5320-1, FHWA, Texas Department of Transportation, 2007.
3. Federal Aviation Administration, Office of Airport Safety and Standards, "Airport Pavement Design and Evaluation", Advisory Circular AC150/5320-6E, 2009.
4. Blotta, F.; Mehta, Y. A.; Clearly, D.; Cunliffe, C.; Joshi, A., "Evaluating the Performance of Doweled and Isolation Joints at the National Airport Pavement Testing Facility," Transportation Research Board Annual Meeting, Washington D.C., pp. 1-15, 2013.
5. Khazanovich, L., *Structural Analysis of Multi-Layered Concrete Pavement Systems*, Ph.D. Thesis, University of Illinois, Urbana-Champaign, IL, 1994.
6. Airbus S.A.S., Technical Data Support and Services, "A300 Airplane Characteristics for Airport Planning", December 2009.
7. Boeing Commercial Airplanes, Office of Airport Technology, "MD-11 Airplane Characteristics for Airport Planning", May 2011.
8. Boeing Commercial Airplanes, Office of Airport Technology, "DC/MD-10 Airplane Characteristics for Airport Planning", May 2011.